

Site-Specific Copper-Catalyzed Oxidation of α -Synuclein: Tightening the Link between Metal Binding and Protein Oxidative Damage in Parkinson's Disease

Marco C. Miotto,^{†,‡} Esaú E. Rodríguez,[§] Ariel A. Valiente-Gabioud,^{†,‡} Valentina Torres-Monserrat,^{†,‡} Andrés Binolfi,^{||} Liliana Quintanar,[§] Markus Zweckstetter,^{⊥, #, ∇} Christian Griesinger,[⊥] and Claudio O. Fernández^{*, †, ‡, §, ||}

[†]Max Planck Laboratory for Structural Biology, Chemistry and Molecular Biophysics of Rosario (MPLbioR), Universidad Nacional de Rosario, 27 de Febrero 210 bis, S2002LRK Rosario, Argentina

[‡]Instituto de Biología Molecular y Celular de Rosario, (IBR-CONICET), Universidad Nacional de Rosario, 27 de Febrero 210 bis, S2002LRK Rosario, Argentina

[§]Centro de Investigación y de Estudios Avanzados (Cinvestav), Av. Instituto Politécnico Nacional 2508, 07360 D.F. México

^{||}In-cell NMR, Department of NMR-supported Structural Biology, Leibniz Institute of Molecular Pharmacology (FMP), Robert-Roessle-Str. 10, 13125 Berlin, Germany

[⊥]Department of NMR-based Structural Biology, Max Planck Institute for Biophysical Chemistry, Am Fassberg 11, D-37077 Göttingen, Germany

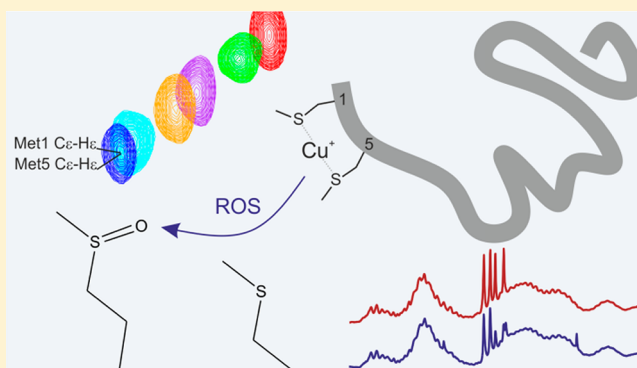
[#]Deutsches Zentrum für Neurodegenerative Erkrankungen (DZNE), 37077 Göttingen, Germany

[∇]Center for Nanoscale Microscopy and Molecular Physiology of the Brain, University Medical Center, 37075 Göttingen, Germany

[¶]SEDIPFAR, Servicio de Descubrimiento, Diseño y Desarrollo Pre-Clinico de Fármacos de la Argentina, Drug Discovery Platform, UNR-CONICET, 27 de Febrero 210 bis, S2002LRK Rosario, Argentina

Supporting Information

ABSTRACT: Amyloid aggregation of α -synuclein (AS) has been linked to the pathological effects associated with Parkinson's disease (PD). Cu^{II} binds specifically at the N-terminus of AS and triggers its aggregation. Site-specific Cu^{I} -catalyzed oxidation of AS has been proposed as a plausible mechanism for metal-enhanced AS amyloid formation. In this study, Cu^{I} binding to AS was probed by NMR spectroscopy, in combination with synthetic peptide models, site-directed mutagenesis, and C-terminal-truncated protein variants. Our results demonstrate that both Met residues in the motif $^1\text{MDVFM}^5$ constitute key structural determinants for the high-affinity binding of Cu^{I} to the N-terminal region of AS. The replacement of one Met residue by Ile causes a dramatic decrease in the binding affinity for Cu^{I} , whereas the removal of both Met residues results in a complete lack of binding. Moreover, these Met residues can be oxidized rapidly after air exposure of the AS- Cu^{I} complex, whereas Met-116 and Met-127 in the C-terminal region remain unaffected. Met-1 displays higher susceptibility to oxidative damage compared to Met-5 because it is directly involved in both Cu^{II} and Cu^{I} coordination, resulting in closer exposure to the reactive oxygen species that may be generated by the redox cycling of copper. Our findings support a mechanism where the interaction of AS with copper ions leads to site-specific metal-catalyzed oxidation in the protein under physiologically relevant conditions. In light of recent biological findings, these results support a role for AS-copper interactions in neurodegeneration in PD.



INTRODUCTION

The misfolding of proteins into a toxic conformation is proposed to be at the molecular foundation of a number of neurodegenerative disorders including Creutzfeldt-Jakob's disease, Alzheimer's (AD), and Parkinson's disease (PD).¹ One common and defining feature of protein misfolding diseases is the formation and deposition of protein aggregates

in various morphologies, including amyloid fibrils.² Neurodegeneration in PD is characterized by the progressive loss of dopaminergic neurons in the *substantia nigra* and by the presence of amyloid fibrillar cytoplasmic aggregates, known as

Received: December 23, 2013

Published: April 11, 2014

Lewy bodies, in multiple brain regions, containing the protein α -synuclein (AS).^{3–5}

AS comprises 107 amino acid residues distributed in three different regions (Figure S1 in the Supporting Information, SI): the N-terminal region, which encompasses residues 1–60, includes the imperfect repeats KTKEGV and is involved in lipid binding;^{6–8} the highly hydrophobic self-aggregating sequence known as NAC (nonamyloid β component, residues 61–95), which initiates fibrillation;⁹ the acidic C-terminal region, which encompasses residues 96–140, is rich in Pro, Asp, and Glu amino acids, and is essential for blocking rapid AS filament assembly.^{10–12} In its monomeric, intrinsically disordered state, the protein is best described as an ensemble of structurally heterogeneous conformations, with no persistent secondary structure and with long-range inter-residue interactions that have been shown to favor aggregation-autoinhibited conformations.^{13–18} These intramolecular contacts in AS are mainly established between the C-terminus and the NAC region (hydrophobic interactions) and between the C- and N-terminal regions (electrostatic interactions).^{13–15}

Although it remains unclear how AS can initiate neuronal death, there is growing evidence that supports a role for AS aggregation in the pathological effects associated with PD.^{19–22} Protein–metal interactions play an important role in AS aggregation and might represent a link between the pathological processes of protein aggregation, oxidative damage in the brain, and neuronal cell loss.^{23–31} The involvement of metal ions in PD was first proposed based on the fact that iron deposits were identified in Lewy bodies³² and elevated copper concentrations were found in the cerebrospinal fluid of PD patients.³³ Furthermore, epidemiological research indicates that individuals with chronic exposure to copper or iron display an increased rate of PD,²⁴ whereas the direct injection of copper in the nigrostriatal system of rats showed that this metal ion seems to induce degeneration by destroying the antioxidant defenses and promoting apoptosis.^{23,34}

Recent biophysical and structural studies demonstrated that the effect of metal ions on AS fibrillation is determined by their binding properties.^{27,31,35–37} Moreover, the strong link between the affinity of metal binding to AS and effectiveness in accelerating AS filament assembly revealed a hierarchy of AS–metal interactions dictated by structural determinants. Overall, the specificity of copper binding to AS indicates that the mechanism through which copper impacts AS aggregation differs significantly from that exerted by other metal ions.^{26,27,35,38,39} Therefore, the coordination chemistry of copper bound to AS has deserved a lot of attention in the past few years.

Most of the studies on the interaction of copper with AS have been aimed at elucidating the coordination environment of Cu^{II} bound to the protein,^{27,39–43} and although some studies have investigated the reactive oxygen species (ROS) reactions catalyzed by the copper complexes, information regarding the structure, affinity, and reactivity of the AS–Cu^I complexes is scarce.²⁷ The occurrence of associated Cu^I/dioxygen chemistry and the description of the binding features of Cu^I to AS have been reported recently.^{44,45} In addition, cyclic voltammetry showed that AS–Cu^I complexes can undergo reoxidation with generation of H₂O₂ and other ROS that are toxic to dopaminergic cultured cells.⁴⁶ Thus, elucidation of the residue-specific basis determining Cu^I coordination to AS is central to establishing a connection of the AS–Cu^I/AS–Cu^{II} structural-affinity features with the mechanistic basis (i.e.,

oxidative damage) behind the metal-enhanced AS amyloid assembly.

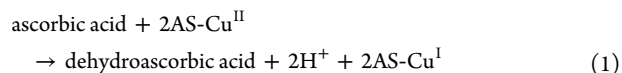
Here we report a detailed structural characterization of Cu^I binding to the ¹MDVFM⁵ sequence in the N-terminal region of AS, identified as the high-affinity copper binding site.⁴⁴ NMR spectroscopy, in combination with site-directed mutagenesis, C-terminal-truncated protein variants, and synthetic peptide models, was used. Our data demonstrate that both Met residues constitute key structural determinants for the preferential binding of Cu^I to the N-terminal region of AS,^{44,47,48} resembling that of the MX₃M motifs in copper-transport proteins. We further showed that the Met residues located in the ¹MDVFM⁵ motif can be oxidized rapidly after Cu^I binding and air-exposure conditions, whereas Met residues at positions 116 and 127 in the C-terminal region of AS remained unaffected under the experimental conditions. Overall, the different oxidation rates observed for Met residues correlated very well with their affinity features for Cu^I.

The high-resolution structural and molecular information emerging from this work demonstrates the occurrence of a site-specific copper-catalyzed oxidation in the protein AS under physiologically relevant conditions, which in the light of recent biological findings supports a role for copper–AS interactions in neurodegeneration in PD.

EXPERIMENTAL SECTION

Proteins and Reagents. The proteins AS and its variants 1-108 H50A AS and 1-108 MSI/H50A AS were prepared as previously described.¹² Purified proteins were dialyzed against buffer A (20 mM MOPS, 100 mM NaCl, pH 7.4), all treated with Chelex (Sigma). Peptide ¹MDVFMK⁶ (PIAS) and its variants ¹IDVFMK⁶ (MII PIAS), ¹MDVFIK⁶ (MSI PIAS), and ¹IDVFIK⁶ (MII/MSI PIAS) were synthesized in the solid phase (Rink amide resin) using Fmoc chemistry. They were purified by reverse-phase high-performance liquid chromatography (HPLC; Waters Delta 600) and characterized by HPLC and electrospray ionization time-of-flight mass spectrometry (ESI-TOF-MS; Agilent; Figure S2 in SI). Peptides were amidated at the C-terminal carboxylate group, while the α -NH₂ terminal was left unmodified. The absorption extinction coefficients of the peptides were determined using a calibration curve prepared in buffer A, weighing out dry peptide samples. The absorption extinction coefficient for all of the peptides used was 11500 cm⁻¹ M⁻¹ at 214 nm and was used to determine the peptide concentration in each sample.

Generation of the Cu^I Complexes. To obtain the Cu^I complexes with AS (50–100 μ M) and peptides (50–300 μ M), the Cu^{II} complexes were first prepared and then reduced with 6–12 and 6–35 mM ascorbic acid, respectively. Ascorbic acid was added from a 0.5 M stock solution. After pH adjustment, samples were treated with a flow of N₂ for 5 min to generate a N₂ atmosphere. The reduction of copper(II) protein/peptide complexes with ascorbic acid, as shown in eq 1, was followed by a decrease of the characteristic d–d transition band in the UV–vis spectrum, as previously described.⁴⁴ Spectra were recorded at 15 °C on a Jasco V-550 spectrophotometer.



Metal-Catalyzed Oxidation. The induction of oxidative damage on peptide and protein samples was monitored by NMR and matrix-assisted laser desorption/ionization time-of-flight (MALDI-TOF) mass spectrometry. NMR spectra of AS–Cu^I complexes were recorded after 2–25 h of air exposure and the addition of 5 mM ethylenediaminetetraacetic acid (EDTA).⁴⁴ For MALDI-TOF analysis, samples were also treated with EDTA and mixed 1:1 with a matrix solution (10 mg/mL of α -cyano-4-hydroxycinnamic acid in 50% aqueous acetonitrile containing 0.1% trifluoroacetic acid).

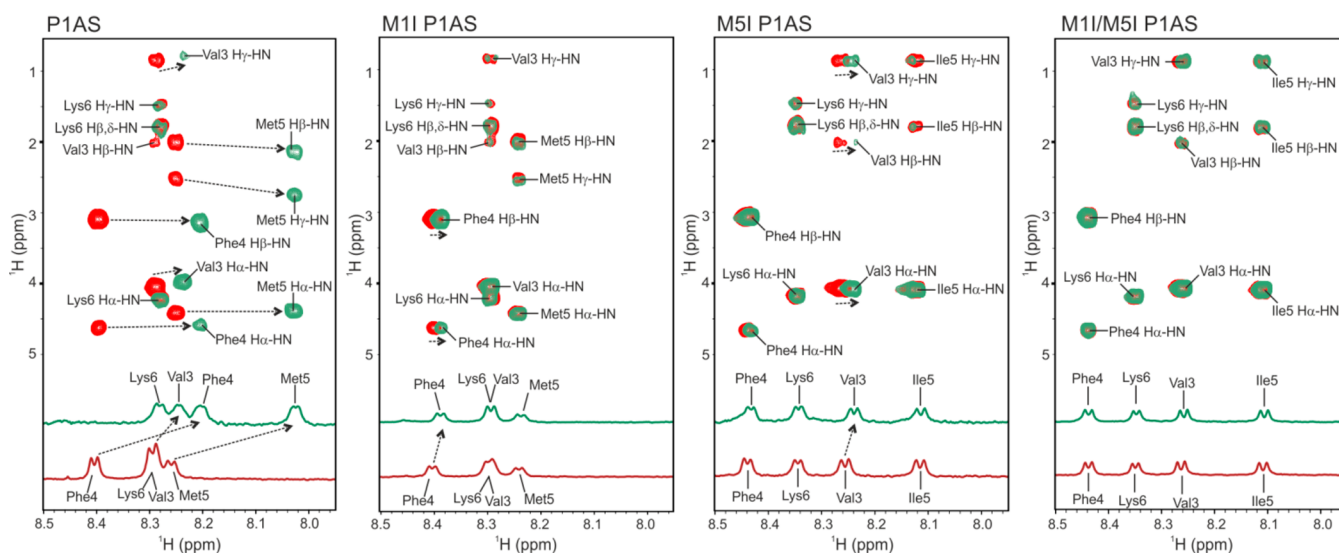
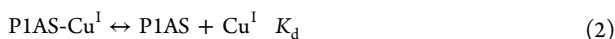


Figure 1. NMR analysis of Cu^{I} binding to AS peptides. Overlaid 2D ^1H – ^1H TOCSY NMR spectra of P1AS, M5I P1AS, M1I P1AS, and M1I/M5I P1AS in the absence (red) and presence (green) of 1 equiv of Cu^{I} . All experiments were recorded on 300 μM peptide samples dissolved in buffer A at 15 $^{\circ}\text{C}$.

NMR Spectroscopy. NMR spectra were acquired on a Bruker Avance II 600 MHz spectrometer using a triple-resonance probe equipped with z-axis self-shielded gradient coils. 2D ^1H – ^{13}C HSQC and ^1H – ^1H TOCSY NMR spectra were registered at 15 $^{\circ}\text{C}$ on 50–100 μM protein (isotopically enriched in ^{13}C) and 50–300 μM peptide samples dissolved in buffer A, in the absence and presence of the metal ion. With the exception of the metal-catalyzed oxidation studies, NMR tubes sealed under a N_2 atmosphere were used in all cases.

^1H – ^{13}C HSQC and ^1H – ^1H TOCSY NMR cross peaks affected during metal titration experiments were identified by comparing their chemical shift values with those of the same cross peaks in the data set of samples lacking metal ion. Differences in the mean weighted chemical shift ($\text{MW}\Delta\text{CS}$) displacements for ^1H and ^{13}C were calculated as $[(\Delta\delta^1\text{H})^2 + (\Delta\delta^{13}\text{C}/4)^2]^{1/2}$.⁴⁹ Acquisition, processing, and visualization of the NMR spectra were performed using *TOPSPIN 2.1* (Bruker) and *Sparky*.

The affinity features of Cu^{I} binding to the different protein and peptide variants were determined from 1D ^1H and 2D ^1H – ^{13}C HSQC NMR experiments on protein/peptide samples recorded at increasing concentrations of the metal ion. Changes in the chemical shift values of amide and aliphatic resonances of Met-1, Val-3, Phe-4, and Met-5 residues were fit to a model incorporating one Cu^{I} ion per molecule, as shown in eq 2 (with apparent dissociation constant K_{d}), using the program *DynaFit*.⁵⁰



The reported K_{d} values assume that disproportionation of Cu^{I} and/or precipitation of $\text{Cu}(\text{OH})$ and Cu_2O did not occur or were extremely low under the experimental conditions of our studies. The absence of line broadening in the NMR spectra, indicative of the formation of paramagnetic Cu^{II} ions or molecular precipitates, supports this assumption.

RESULTS

Structure-Affinity Determinants of the High-Affinity Cu^{I} Binding Site in AS. The details of Cu^{I} binding to the $^1\text{MDVFM}^5$ motif in the N-terminal region of AS (site 1), identified as the high-affinity copper binding site,⁴⁴ were explored at single-residue resolution using NMR spectroscopy. In order to assess the role of methionine residues (Met) in metal complexation to the site, we first compared the binding

features of Cu^{I} to the synthetic peptide $^1\text{MDVFMK}^6$ (P1AS) and the variants M1I P1AS, M5I P1AS, and M1I/M5I P1AS. These Ile variants were used as Met mimics that lack metal-coordinating capabilities because of the absence of the sulfur atom.

The backbone amide regions of 1D ^1H and 2D ^1H – ^1H TOCSY NMR spectra of the P1AS variants in the absence and presence of Cu^{I} are shown in Figure 1. Although the amide resonances of Met-1 and Asp-2 cannot be detected in these experiments because of solvent-exchange effects, the spectral region contains well-resolved spin systems for the other residues and thus constitutes an excellent probe to analyze the interaction process. As reflected by Figure 1, the 1D and 2D resonances assigned to the amide proton of Phe-4 and Met-5 of P1AS were the most affected by the presence of the metal ion. The resonance corresponding to the amide proton of Val-3 was also affected, although to a lesser extent, whereas no changes in the signals belonging to Lys-6 were observed. On the contrary, the effects of Cu^{I} binding were less pronounced in the peptide variants lacking one of the Met residues. In those cases, only a small shifting of the Val-3 and Phe-4 resonances was detectable because of Cu^{I} complexation with the M5I P1AS and M1I P1AS peptides, respectively (Figure 1). In all cases, the addition of EDTA abolished the changes induced by the metal ion, confirming the reversibility of the interaction (data not shown). Finally, we noted the lack of interaction of Cu^{I} with the double mutant peptide M1I/M5I P1AS, demonstrating the complete loss of Cu^{I} binding to site 1 of AS upon the replacement of both methionine residues in the sequence by isoleucine. Moreover, the absence of line broadening in the NMR signals of this double mutant demonstrates that all of the copper added is in the Cu^{I} state under the experimental conditions of our studies.

We further characterized the interaction of Cu^{I} with P1AS and the mutant variants by inspecting the aliphatic and methyl regions in the corresponding NMR spectra (Figure 2). The 1D ^1H NMR experiments shown in Figure 2 indicate clearly that the degree of perturbation induced by Cu^{I} on the S-CH_3 resonances of the Met-1 and Met-5 residues decrease substantially in the variants M1I P1AS and M5I P1AS

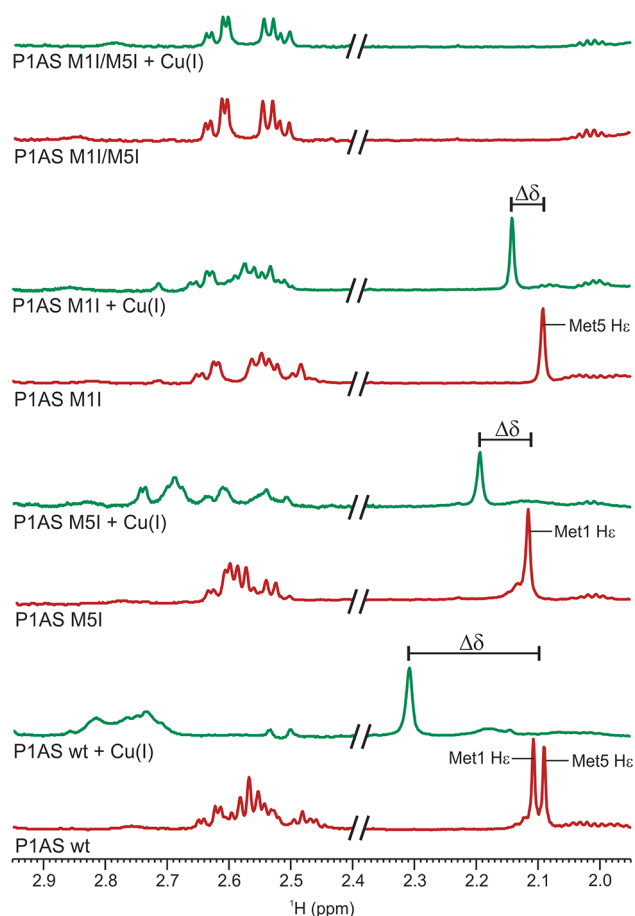


Figure 2. NMR analysis of Cu^{I} binding to AS peptides. 1D ^1H NMR spectra (2.0–2.9 ppm) of AS peptides in the absence (red) and presence (green) of 1 equiv of Cu^{I} . Changes in the chemical shifts ($\Delta\delta$) corresponding to the H_ϵ protons in the $\text{S}-\text{CH}_3$ groups of the Met-1 and Met-5 residues are identified (2.0–2.4 ppm). In addition, the spectral regions of H_γ protons of Met residues in their uncomplexed and complexed forms are also shown (2.4–2.9 ppm). All experiments were recorded on 300 μM peptide samples dissolved in buffer A at 15 $^\circ\text{C}$.

compared to the P1AS peptide. These results confirm that the effects observed on the amide groups of the P1AS species in the presence of Cu^{I} reflect the direct interaction of the metal ion with the sulfur atoms of the Met-1 and Met-5 residues, consistent with the binding preferences of Cu^{I} to the sulfur atoms of the Met residues in metalloproteins. Altogether, our data allow us to conclude that the presence of both Met residues is key to the binding of Cu^{I} to site 1 because coordination of Cu^{I} to that site is strongly reduced upon replacement of one of the Met residues, whereas a complete loss of metal binding is observed when both Met residues are absent.

To assess the impact of Met replacement on the affinity features of Cu^{I} binding to site 1, we determined the dissociation constants of Cu^{I} complexed to P1AS and its variants using chemical shift data from the 1D ^1H and 2D $^1\text{H}-^1\text{H}$ TOCSY NMR experiments. The resonances corresponding to the $\text{S}-\text{CH}_3$ groups of Met-1 and Met-5, the backbone amide proton of Met-5, and the H_γ proton of Val-3 and H_3-H_5 protons of Phe-4 are all well-resolved over the entire Cu^{I} titration experiments and thus well-suited for calculation of the dissociation constant (K_d). Figure 3 shows the binding curves

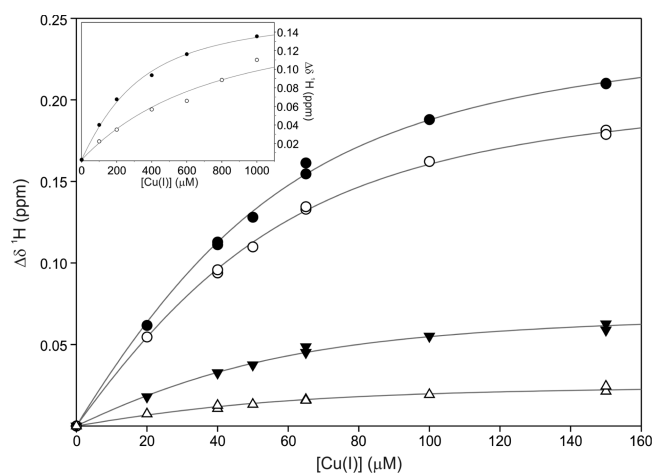


Figure 3. Affinity features of Cu^{I} binding to AS peptides. The panel shows the binding curves of Cu^{I} to P1AS (50 μM), as monitored by changes in the chemical shifts ($\Delta\delta^{\text{1H}}$) of the H_ϵ protons of Met-1 and Met-5 (○), the H_γ proton of Val-3 (Δ), the H_3-H_5 protons of Phe-4 (▼), and the HN proton of Met-5 (●). The inset shows the binding curves of Cu^{I} to M5I P1AS and M11 P1AS (200 μM), as monitored by changes in the chemical shifts ($\Delta\delta^{\text{1H}}$) of the H_ϵ protons of Met-1 (●) and the H_ϵ protons of Met-5 (○), respectively. Curves represent the fit to the models described in the text, using the program *DynaFit*. All experiments were recorded on peptide samples dissolved in buffer A at 15 $^\circ\text{C}$.

of Cu^{I} to P1AS and the variants M11 P1AS and M5I P1AS. The NMR-derived apparent affinity for the complex of Cu^{I} with P1AS was $20 \pm 2 \mu\text{M}$, whereas values of 200 ± 20 and $>500 \mu\text{M}$ were estimated from the data measured for the M5I P1AS and M11 P1AS variants, respectively.

To confirm the findings derived from our analysis of Cu^{I} binding to peptide models, we then analyzed the structural and affinity features of the Cu^{I} complex with the $^1\text{MDVFM}^5$ motif in the N-terminal region of the protein AS. To this purpose, we used ^{13}C isotopically enriched H50A and M5I/H50A mutants of the C-terminal-truncated (aa1-108) AS protein. Instead of the full length protein, we chose to study these variants because the presence of the lower-affinity His50 and C-terminal Cu^{I} binding sites unnecessarily crowds the spectral region under study and complicates analysis. The $^1\text{H}-^{13}\text{C}$ correlations corresponding to the $\gamma-\text{CH}_2$ and $\text{S}-\text{CH}_3$ groups of the Met residues in the $^1\text{MDVFM}^5$ sequence were detected by 2D $^1\text{H}-^{13}\text{C}$ HSQC NMR experiments, and their chemical shifts were measured in the absence and presence of increasing concentrations of Cu^{I} ions (Figure 4). From these experiments, the NMR-derived affinity for the complex of Cu^{I} with the H50A 1-108 AS variant was $17 \pm 2 \mu\text{M}$, whereas a value of $190 \pm 30 \mu\text{M}$ was estimated from the data measured for the M5I/H50A 1-108 AS mutant. Overall, these data demonstrate that the structure-affinity determinants for Cu^{I} binding observed in the synthetic peptide models are preserved in the protein.

Site-Specific Copper-Catalyzed Oxidation of AS.

Because Met residues are one of the preferred targets in proteins under conditions of site-specific metal-catalyzed oxidation, we also investigated the occurrence of oxidative damage in Cu^{I} -bound AS samples under aerobic conditions, followed by treatment with EDTA. The protein AS contains four Met residues distributed in the N-terminal (Met-1 and Met-5) and C-terminal (Met-116 and Met-127) regions, whose $\text{S}-\text{CH}_3$ (H_ϵ) proton resonances were assigned unambiguously

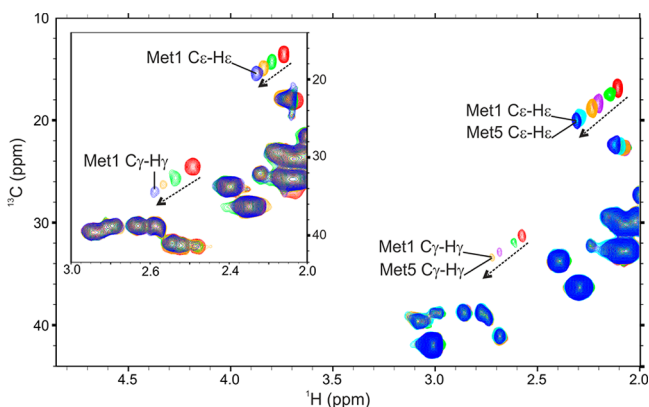


Figure 4. NMR analysis of Cu^{I} binding to the protein AS. Overlaid ^1H - ^{13}C HSQC NMR spectra of 1-108 H50A AS ($50 \mu\text{M}$) in the presence of increasing Cu^{I} concentrations: red ($0 \mu\text{M}$), green ($10 \mu\text{M}$), purple ($20 \mu\text{M}$), orange ($50 \mu\text{M}$), cyan ($75 \mu\text{M}$), and blue ($150 \mu\text{M}$). The inset shows the overlaid ^1H - ^{13}C HSQC NMR spectra of 1-108 MSI/H50A AS ($100 \mu\text{M}$) in the presence of increasing Cu^{I} concentrations: red ($0 \mu\text{M}$), green ($50 \mu\text{M}$), orange ($300 \mu\text{M}$), and blue ($450 \mu\text{M}$). All experiments were recorded in buffer A at 15°C .

by comparing the 1D ^1H NMR spectra of the different protein and peptide variants studied in this work (Figure 5A). Upon complexation with Cu^{I} and air exposure, a substantial decrease

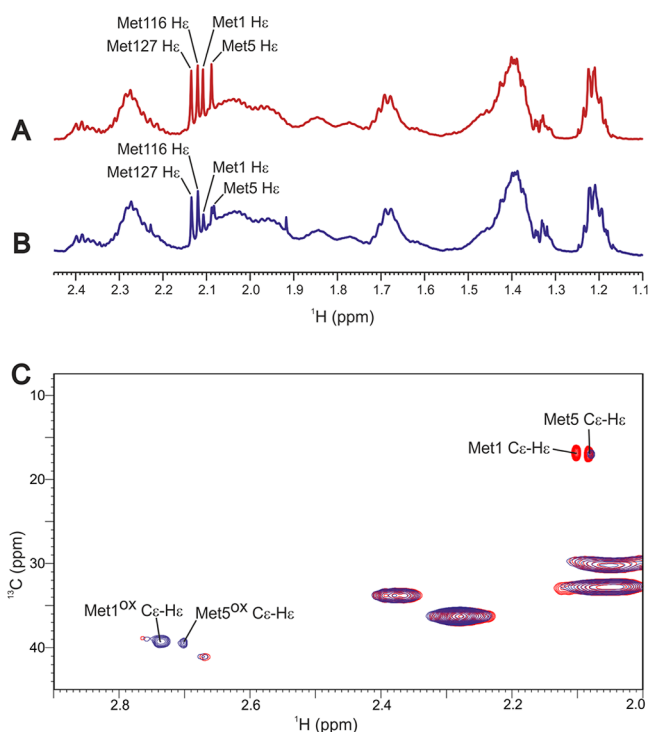


Figure 5. Copper-mediated oxidation of AS. 1D ^1H NMR spectra of AS ($100 \mu\text{M}$) in the absence (A) and presence (B) of 1 equiv of Cu^{I} , followed by 5 h of air exposure and the addition of 5 mM EDTA. Signals corresponding to the H_ϵ protons of the methyl groups of Met residues at the N- and C-terminal regions are identified. (C) Overlaid ^1H - ^{13}C HSQC NMR spectra of 1-108 H50A AS ($100 \mu\text{M}$) in the unmodified (blue) and oxidized (red) forms. The changes in the intensities of the ^1H - ^{13}C correlations of $\text{S}-\text{CH}_3$ groups indicate that copper-catalyzed oxidation of Met-1 is faster than that of Met-5. NMR experiments were recorded in buffer A at 15°C , after the addition of 5 mM EDTA.

in the intensity of the signals of the $\text{S}-\text{CH}_3$ groups of the N-terminal Met residues was observed in AS samples treated with EDTA, compared to metal-free protein samples. In contrast, $\text{S}-\text{CH}_3$ resonances of the C-terminal Met residues remained almost unaffected (Figure 5B). Although a decay in the intensity of the N-terminal Met resonances might be indicative of the occurrence of oxidative damage at the Met-1 and Met-5 positions of AS, the severe signal overlapping that characterizes the 1D ^1H NMR spectra of protein samples did not allow us to identify a new set of resonances derived from oxidized methionine residues.

To gain further insight into the mechanistic basis behind the changes observed by 1D NMR, we performed ^1H - ^{13}C 2D HSQC NMR experiments on the ^{13}C isotopically labeled C-terminal-truncated form of AS bearing the H50A mutation. The ^1H - ^{13}C correlations belonging to the $\text{S}-\text{CH}_3$ groups of the Met-1 and Met-5 residues in their free, metal-complexed, and oxidized states were well-resolved and could be assigned unambiguously (Figure 5C). The experiments clearly showed the appearance of new resonances at ^1H and ^{13}C chemical shifts that are typical of $\text{S}-\text{CH}_3$ groups of methionine residues in their sulfoxide form (Figure 5C),^{51,52} in tandem with attenuation of the methyl correlations of residues Met-1 and Met-5 in its unmodified, metal-free form. Methionine oxidation to sulfoxide was further confirmed by MALDI-TOF analysis for MII P1AS and MSI P1AS (Figure S3 in the SI), as was previously reported for the P1AS peptide.⁴⁴ Interestingly, comparative analysis of the intensities of the Met-1 and Met-5 resonances before and after air-exposure conditions points to a much faster oxidation of Met-1. Indeed, at the end point of our experiment, we could still detect the H_ϵ - C_ϵ cross peak corresponding to unoxidized Met-5 ($\sim 15\%$), while that of Met-1 had completely vanished (Figure 5C).

To shed more light onto the details of the AS oxidation process, we then studied the time-dependent oxidation of the Cu^{I} -complexed forms of the P1AS, MSI P1AS, and MII P1AS peptides under aerobic conditions. The intensities of the $\text{S}-\text{CH}_3$ resonances of methionine in its sulfoxide forms were used to obtain semiquantitative data (Figure S4 in the SI). From inspection of the $\text{S}-\text{CH}_3$ resonances of the P1AS peptide, it became evident that oxidation of Met-1 and Met-5 is complete after 24 h of air exposure (Figure 6A). However, time-resolved analysis revealed that the oxidation rate is at least two times faster for Met-1 ($t_{1/2} \sim 7 \text{ h}$) than for Met-5 ($t_{1/2} \sim 15 \text{ h}$; Figure 6A,B). In contrast, the results obtained from analysis of the MSI P1AS and MII P1AS variants after 24 h of incubation showed that oxidation only progresses up to 40% and 10%, respectively (Figure S5 in the SI).

DISCUSSION

The details of Cu^{I} binding to the high-affinity interface of AS were studied by NMR spectroscopy, in combination with synthetic peptide models, site-directed mutagenesis, and C-terminal-truncated protein variants designed especially for this purpose. Our results demonstrate conclusively that both Met residues in the motif $^1\text{MDVFM}^5$ are key to the high-affinity binding of Cu^{I} to the N-terminal region of AS, consistent with the preference of the soft cation Cu^{I} for sulfur ligands.^{48,53} Indeed, when we replaced one Met residue by nonsulfur amino acids as in the MII and MSI variants, the affinity for the interaction decreased dramatically, whereas the removal of both Met residues resulted in the complete lack of binding. These results are in full agreement with previous reports aimed to

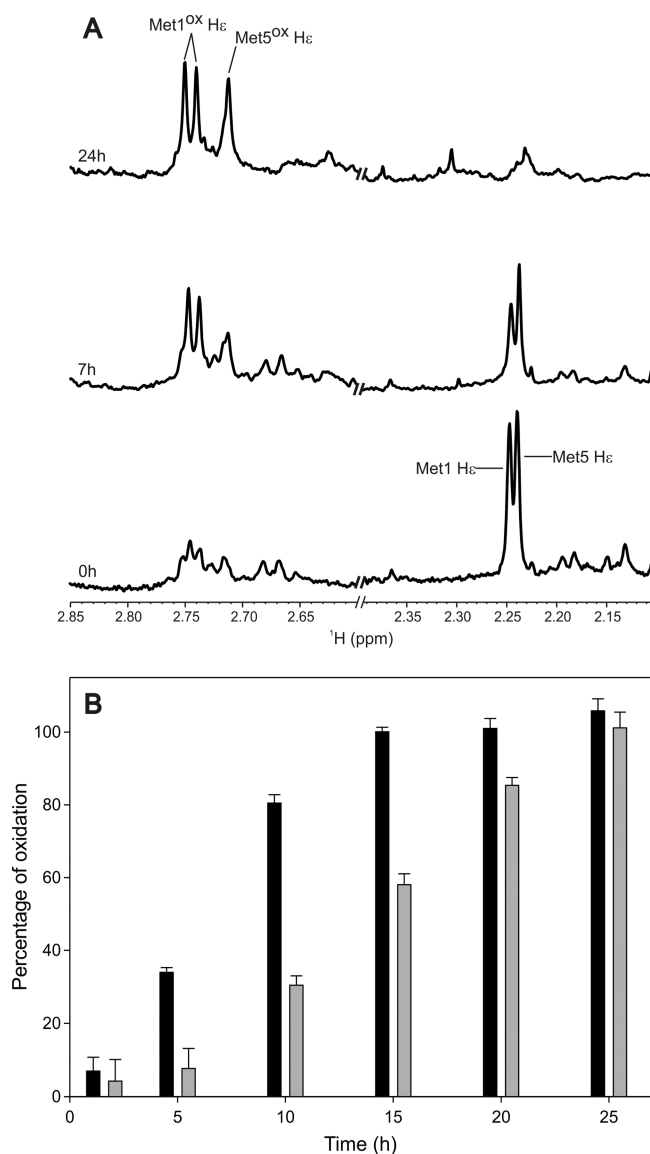


Figure 6. Metal-catalyzed oxidation of the PIAS peptide monitored by NMR. (A) Time evolution of 1D ^1H NMR spectra of the PIAS peptide in the presence of 1 equiv of Cu^{I} under aerobic conditions. Detection of a doublet for oxidized Met-1 H ϵ protons is due to the presence of the R and S diastereoisomers, as previously reported.^{77,78} (B) Oxidation of Met residues as a function of time monitored by integrating the signals corresponding to the H ϵ protons of Met-1 (black bars) and Met-5 (gray bars) in their sulfoxide states. All experiments were recorded on 100 μM peptide samples dissolved in buffer A at 15 $^\circ\text{C}$.

understand the Cu^{I} binding features of Met-only sites, where interaction with the metal ion occurs exclusively via coordination of the thioether groups.⁴⁷ Using model peptides mimicking the sequences of the yeast Cu^{I} transporter Ctr1 and the bacterial copper-resistant protein PcoC, those studies showed that sequences of the type MTGMKGMS were able to coordinate Cu^{I} , with dissociation constants ranging between 2 and 11 μM , in a coordination arrangement that involves the sulfur atoms of three Met residues.⁴⁷ Interestingly, the removal of one of these Met residues resulted in a Met(S)- Cu^{I} -(S)Met complex with weaker affinity features, in the 20–40 μM range. The comparable affinities for the Met(S)- Cu^{I} -(S)Met complex in Met-only coordination peptides and the one reported in our

work for the Cu^{I} binding sequence $^1\text{MDVFM}^5$ indicate that Cu^{I} binding to PIAS likely occurs exclusively via the Met-1 and Met-5 sulfur atoms. Although human AS has been proposed to be predominantly acetylated at the N terminus *in vivo*, no substantial changes in the Cu^{I} binding features of the protein are expected to occur according to the coordination properties reported here. Further support for the formation of a Met(S)- Cu^{I} -(S)Met complex arises from the fact that mapping of the PIAS- Cu^{I} interaction through chemical shift measurements revealed that major changes were centered at the H γ and H ϵ protons of the Met-1 and Met-5 residues (Figure S6 in the SI), consistent with a previous study where Ag^{I} was used as a probe for Cu^{I} binding at the N terminus of AS.⁵⁴

The K_{d} values measured here indicate a low binding affinity of AS for Cu^{I} ; however, the intracellular environment may provide the conditions for copper ions to be complexed by AS. Indeed, AS is abundantly expressed in the brain, and local intracellular concentrations in the range of ~ 20 – $100 \mu\text{M}$ have been reported.^{55,56} Additionally, intracellular copper concentrations can reach up to 15 μM in brain synaptosomes and $\sim 300 \mu\text{M}$ in synaptic vesicles,^{57,58} where AS is enriched.⁵⁹ These concentrations might be even higher under pathological conditions where the normal metabolism of copper would be perturbed, as reported for several neurodegenerative disorders.²⁹ Although the concentration of free intracellular copper is expected to be very low because of its coordination to metalloproteins and chaperones, there is growing evidence for the presence of a pool of dynamic copper ions that are loosely bound to different metabolites and could become available to interact with AS.^{60,61} Finally, copper-transport proteins, such as Ctr1, that coordinate Cu^{I} via Met-only sites at the membrane show binding affinities in the same order as those reported here for AS.^{47,48} Overall, these works suggest that conditions could be met for the formation of AS- Cu^{I} complexes in the intracellular environment.

As reported by several co-workers, oxidative modifications of AS were proposed to play a role in its amyloid aggregation and numerous studies were devoted to understanding the structural and cellular consequences of AS oxidation.^{62,63} In the particular case of Met-involved oxidation, it was suggested that this modification inhibits amyloid fibril formation but promotes the formation of stable AS oligomers.^{64–68} In addition, a recent work by Bax and collaborators demonstrated that the lipid-mediated oxidation of AS at the Met-1 and Met-5 residues substantially affected the membrane-binding properties of the protein.⁶⁹ Added to the fact that oxidation of AS is able to inhibit the degradation of oligomers by the autophagy pathway,^{62,70} this evidence was used to hypothesize that oxidation of AS at Met residues might lead to an increase in the concentration of cytosolic AS that could readily oligomerize.⁶³ Moreover, from the pool of cytosolic enzymes that are involved in the repair of methionine sulfoxide modifications^{63,71,72}—MsrA and MsrB—the MsrA enzyme was able to repair efficiently only those oxidative modifications affecting Met-5, being almost inactive against the Met-1 sulfoxide form of AS.⁶⁹ This biological evidence indicates that a complex balance of AS species might exist in cells under oxidative conditions, and thus knowledge of the mechanistic basis behind the formation of such species is key to understanding the molecular events leading to amyloid aggregation of AS in PD.

To shed light onto the role that metal-catalyzed oxidation might have in the formation of the oxidized species referred to above, we also studied the copper-mediated oxidation of AS. In

our studies, we used ascorbic acid as the reducing agent because (a) ascorbic acid was shown to be an efficient reductant of Cu^{II} sites in metalloenzymes and amyloidogenic proteins,^{47,73} (b) according to the redox potential of the AS-Cu^{II} complex reported recently ($E = 0.018 \text{ V}$ vs Ag/AgCl), it was demonstrated that ascorbic acid ($E = -0.145 \text{ V}$ vs Ag/AgCl) can directly reduce AS-Cu^{II} to AS-Cu^{I} ,⁴⁴ and (c) high levels of ascorbic acid were reported in the intracellular milieu of neurons.^{74,75} Our experiments demonstrated that the formation of AS–copper complexes in the low micromolar range, under conditions that favor the redox cycle of the $\text{Cu}^{\text{I}}/\text{Cu}^{\text{II}}$ couple, led to the selective oxidation of Met-1 and Met-5 residues, while no significant oxidation of the C-terminal Met residues was observed. These results reflect the preferential binding of copper ions to the N-terminal region of AS compared to the negatively charged C-terminal interface,^{35,40,44} indicating that under the experimental conditions of our studies only the N-terminal sites involving Met-1 and Asp-2 for Cu^{II} binding and Met-1 and Met-5 for Cu^{I} binding would be significantly populated. The observed results are also consistent with the well-known susceptibility of the Met residues to oxidation, and the transient nature of the ROS generated by the redox cycle of copper ions, capable of oxidizing only amino acids in the vicinity of the metal complex.

Overall, our results indicate that the oxidation rate of Met residues was strongly reduced in the M11 P1AS and MSI P1AS variants compared to the P1AS peptide containing the sequence $^1\text{MDVFM}^5$ (Figure S5 in the SI). In particular, in the $^1\text{MDVFM}^5$ motif, the Met-1 residue proved to be more susceptible to oxidation than Met-5, as shown in Figure 6. Whereas the different oxidation rates observed for Met residues in the peptide variants—P1AS > MSI P1AS \gg M11 P1AS—correlate very well with their affinity features for Cu^{I} , the higher susceptibility of Met-1 to oxidative damage compared to Met-5 in the P1AS peptide could be explained on the basis that Met-1 is directly involved in both Cu^{II} and Cu^{I} coordination, resulting in a closer exposure to the ROS generated by the redox cycling of copper in the metal sites. Moreover, the high susceptibility of Met-1 to oxidation might reflect the existence of a redox-active AS-Cu^{I} state populated by a transient conformer in which interaction of Met-1 with the metal ion is strongly favored. Indeed, the formation of a redox-active, low-populated $\text{A}\beta\text{-Cu}^{\text{I}}$ conformer that is able to undergo fast electron transfer and catalyzes ROS production was reported very recently.⁷⁶ The coordination chemistry of that redox-active $\text{A}\beta\text{-Cu}^{\text{I}}$ was shown to be different from the highest populated $\text{A}\beta\text{-Cu}^{\text{I}}$ conformer, whereas the transient character of this state explained why it was not detected through spectroscopic studies of $\text{A}\beta\text{-Cu}^{\text{I}}$ and $\text{A}\beta\text{-Cu}^{\text{II}}$.⁷⁶ This might be also true for AS; however, further studies are clearly needed to elucidate the molecular basis of the differences observed in the time-dependent oxidation of the Met-1 and Met-5 residues.

Our findings and those reported previously support a mechanism through which the interaction of AS with copper ions, in the presence of a physiological electron source such as ascorbic acid, might lead to oxidative damage of the Met-1 and Met-5 residues, prevention of AS–membrane interactions, and accumulation of a pool of AS molecules with an increased tendency to aggregate. The fact that the Met-1 residue is preferentially oxidized by the copper/ascorbic acid system, together with the observation that it is a poor substrate for the methionine sulfoxide reductase MsrA ,⁶⁹ further suggests that copper binding at the N terminus of AS might have an

important impact on AS associated neurodegeneration and the development of PD.

■ ASSOCIATED CONTENT

📄 Supporting Information

Primary sequence of AS, ESI-TOF-MS and HPLC data on P1AS peptides used in this study, MALDI-TOF analysis for M11 P1AS and MSI P1AS after oxidation of their corresponding Cu^{I} complexes, ^1H NMR spectra of oxidized P1AS, MSI P1AS, and M11 P1AS variants, and ^1H – ^{13}C MW Δ CS displacements of P1AS in the presence of Cu^{I} . This material is available free of charge via the Internet at <http://pubs.acs.org>.

■ AUTHOR INFORMATION

Corresponding Author

*E-mail: fernandez@ibr.gov.ar or cfernan@gwdg.de. Phone: +54 341 4448745. Fax: ++54 341 4390465.

Notes

The authors declare no competing financial interest.

■ ACKNOWLEDGMENTS

C.O.F. thanks ANPCyT, FONCyT, CONICET, the Ministry of Education of Argentina, the Ministry of Health of Argentina, the Max Planck Society, and the Alexander von Humboldt Foundation for financial support. C.O.F. is the Head of the Max Planck Laboratory for Structural Biology, Chemistry and Molecular Biophysics of Rosario (MPLbioR), partner of the Max Planck Institute for Biophysical Chemistry (Göttingen). L.Q. and E.E.R. thank the National Council for Science and Technology in Mexico (CONACYT) for financial support (Grant 128255 to L.Q. and a fellowship to E.E.R.). M.C.M. is a recipient of a fellowship from CONICET in Argentina.

■ REFERENCES

- (1) Dobson, C. M. *Semin. Cell Dev. Biol.* **2004**, *15*, 3–16.
- (2) Chiti, F.; Dobson, C. M. *Annu. Rev. Biochem.* **2006**, *75*, 333–366.
- (3) Forno, L. S. J. *Neuropathol. Exp. Neurol.* **1996**, *55*, 259–272.
- (4) Goedert, M. *Nat. Rev. Neurosci.* **2001**, *2*, 492–501.
- (5) Spillantini, M. G.; Schmidt, M. L.; Lee, V. M.; Trojanowski, J. Q.; Jakes, R.; Goedert, M. *Nature* **1997**, *388*, 839–840.
- (6) Bisaglia, M.; Tessari, I.; Pinato, L.; Bellanda, M.; Giraud, S.; Fasano, M.; Bergantino, E.; Bubacco, L.; Mammi, S. *Biochemistry* **2005**, *44*, 329–339.
- (7) Chandra, S.; Chen, X.; Rizo, J.; Jahn, R.; Südhof, T. C. *J. Biol. Chem.* **2003**, *278*, 15313–15318.
- (8) Jao, C. C.; Der-Sarkissian, A.; Chen, J.; Langen, R. *Proc. Natl. Acad. Sci. U.S.A.* **2004**, *101*, 8331–8336.
- (9) Giasson, B. I.; Murray, I. V.; Trojanowski, J. Q.; Lee, V. M. *J. Biol. Chem.* **2001**, *276*, 2380–2386.
- (10) Crowther, R. A.; Jakes, R.; Spillantini, M. G.; Goedert, M. *FEBS Lett.* **1998**, *436*, 309–312.
- (11) Fernández, C. O.; Hoyer, W.; Zweckstetter, M.; Jares-Erijman, E. A.; Subramaniam, V.; Griesinger, C.; Jovin, T. M. *EMBO J.* **2004**, *23*, 2039–2046.
- (12) Hoyer, W.; Cherny, D.; Subramaniam, V.; Jovin, T. M. *Biochemistry* **2004**, *43*, 16233–16242.
- (13) Bertocini, C. W.; Jung, Y.-S.; Fernandez, C. O.; Hoyer, W.; Griesinger, C.; Jovin, T. M.; Zweckstetter, M. *Proc. Natl. Acad. Sci. U.S.A.* **2005**, *102*, 1430–1435.
- (14) Dedmon, M. M.; Lindorff-Larsen, K.; Christodoulou, J.; Vendruscolo, M.; Dobson, C. M. *J. Am. Chem. Soc.* **2005**, *127*, 476–477.
- (15) Lee, J. C.; Gray, H. B.; Winkler, J. R. *J. Am. Chem. Soc.* **2005**, *127*, 16388–16389.

- (16) Lee, J. C.; Lai, B. T.; Kozak, J. J.; Gray, H. B.; Winkler, J. R. *J. Phys. Chem. B* **2007**, *111*, 2107–2112.
- (17) Herrera, F. E.; Chesi, A.; Paleologou, K. E.; Schmid, A.; Munoz, A.; Vendruscolo, M.; Gustincich, S.; Lashuel, H. A.; Carloni, P. *PLoS One* **2008**, *3* (10), e3394.
- (18) Losasso, V.; Pietropaolo, A.; Zannoni, C.; Gustincich, S.; Carloni, P. *Biochemistry* **2011**, *50*, 6994–7001.
- (19) Lashuel, H. A.; Overk, C. R.; Oueslati, A.; Masliah, E. *Nat. Rev. Neurosci.* **2013**, *14*, 38–48.
- (20) Goedert, M.; Spillantini, M. G.; Del Tredici, K.; Braak, H. *Nat. Rev. Neurol.* **2013**, *9*, 13–24.
- (21) Choi, B.-K.; Choi, M.-G.; Kim, J.-Y.; Yang, Y.; Lai, Y.; Kweon, D.-H.; Lee, N. K.; Shin, Y.-K. *Proc. Natl. Acad. Sci. U.S.A.* **2013**, *110*, 4087–4092.
- (22) Irwin, D. J.; Lee, V. M.-Y.; Trojanowski, J. Q. *Nat. Rev. Neurosci.* **2013**, *14*, 626–636.
- (23) Youdim, M. B.; Ben-Shachar, D.; Riederer, P. *Eur. Neurol.* **1991**, *31* (Suppl1), 34–40.
- (24) Yu, W.-R.; Jiang, H.; Wang, J.; Xie, J.-X. *Neurosci. Bull.* **2008**, *24*, 73–78.
- (25) Uversky, V. N.; Li, J.; Fink, A. L. *J. Biol. Chem.* **2001**, *276*, 44284–44296.
- (26) Rasia, R. M.; Bertoncini, C. W.; Marsh, D.; Hoyer, W.; Cherny, D.; Zweckstetter, M.; Griesinger, C.; Jovin, T. M.; Fernández, C. O. *Proc. Natl. Acad. Sci. U.S.A.* **2005**, *102*, 4294–4299.
- (27) Binolfi, A.; Quintanar, L.; Bertoncini, C. W.; Griesinger, C.; Fernández, C. O. *Coord. Chem. Rev.* **2012**, *256*, 2188–2201.
- (28) Wright, J. A.; Wang, X.; Brown, D. R. *FASEB J.* **2009**, *23*, 2384–2393.
- (29) Gaggelli, E.; Kozłowski, H.; Valensin, D.; Valensin, G. *Chem. Rev.* **2006**, *106*, 1995–2044.
- (30) Wang, X.; Moualla, D.; Wright, J. A.; Brown, D. R. *J. Neurochem.* **2010**, *113*, 704–714.
- (31) Binolfi, A.; Fernández, C. O. Interactions of α -Synuclein with Metal Ions: New Insights into the Structural Biology and Bioinorganic Chemistry of Parkinson's Disease. *Brain Diseases and Metalloproteins*; CRC Press, 2012
- (32) Castellani, R. J.; Siedlak, S. L.; Perry, G.; Smith, M. A. *Acta Neuropathol.* **2000**, *100*, 111–114.
- (33) Pall, H.; Blake, D.; Williams, A.; Lunec, J. *Lancet* **1987**, *330*, 596–599.
- (34) Yu, W. H.; Matsuoka, Y.; Sziráki, I.; Hashim, A.; LaFrancois, J.; Sershen, H.; Duff, K. E. *Neurochem. Res.* **2008**, *33*, 902–911.
- (35) Binolfi, A.; Rasia, R. M.; Bertoncini, C. W.; Ceolin, M.; Zweckstetter, M.; Griesinger, C.; Jovin, T. M.; Fernández, C. O. *J. Am. Chem. Soc.* **2006**, *128*, 9893–9901.
- (36) Lamberto, G. R.; Torres-Monserrat, V.; Bertoncini, C. W.; Salvatella, X.; Zweckstetter, M.; Griesinger, C.; Fernández, C. O. *J. Biol. Chem.* **2011**, *286*, 32036–32044.
- (37) Valiente-Gabioud, A. A.; Torres-Monserrat, V.; Molina-Rubino, L.; Binolfi, A.; Griesinger, C.; Fernández, C. O. *J. Inorg. Biochem.* **2012**, *117*, 334–341.
- (38) Lee, J. C.; Gray, H. B.; Winkler, J. R. *J. Am. Chem. Soc.* **2008**, *130*, 6898–6899.
- (39) Binolfi, A.; Rodriguez, E. E.; Valensin, D.; D'Amelio, N.; Ippoliti, E.; Obal, G.; Duran, R.; Magistrato, A.; Pritsch, O.; Zweckstetter, M.; Valensin, G.; Carloni, P.; Quintanar, L.; Griesinger, C.; Fernández, C. O. *Inorg. Chem.* **2010**, *49*, 10668–10679.
- (40) Binolfi, A.; Lamberto, G. R.; Duran, R.; Quintanar, L.; Bertoncini, C. W.; Souza, J. M.; Cerveñansky, C.; Zweckstetter, M.; Griesinger, C.; Fernández, C. O. *J. Am. Chem. Soc.* **2008**, *130*, 11801–11812.
- (41) Jackson, M. S.; Lee, J. C. *Inorg. Chem.* **2009**, *48*, 9303–9307.
- (42) Drew, S. C.; Leong, S. L.; Pham, C. L. L.; Tew, D. J.; Masters, C. L.; Miles, L. A.; Cappai, R.; Barnham, K. J. *J. Am. Chem. Soc.* **2008**, *130*, 7766–7773.
- (43) Kowalik-Jankowska, T.; Rajewska, A.; Jankowska, E.; Grzonka, Z. *Dalton Trans.* **2006**, 5068–5076.
- (44) Binolfi, A.; Valiente-Gabioud, A. A.; Duran, R.; Zweckstetter, M.; Griesinger, C.; Fernandez, C. O. *J. Am. Chem. Soc.* **2011**, *133*, 194–196.
- (45) Lucas, H. R.; DeBeer, S.; Hong, M.-S.; Lee, J. C. *J. Am. Chem. Soc.* **2010**, *132*, 6636–6637.
- (46) Wang, C.; Liu, L.; Zhang, L.; Peng, Y.; Zhou, F. *Biochemistry* **2010**, *49*, 8134–8142.
- (47) Jiang, J.; Nadas, I. A.; Kim, M. A.; Franz, K. J. *Inorg. Chem.* **2005**, *44*, 9787–9794.
- (48) Rubino, J. T.; Riggs-Gelasco, P.; Franz, K. J. *J. Biol. Inorg. Chem.* **2010**, *15*, 1033–1049.
- (49) Cavanagh, J.; Fairbrother, W. J.; Palmer, A.; Rance, M.; Skelton, N. J. *Protein NMR Spectroscopy: Principles and Practice*, 2nd ed.; Elsevier Academic Press: Burlington, MA, 2007.
- (50) Kuzmic, P. *Anal. Biochem.* **1996**, *237*, 260–273.
- (51) Nadal, R. C.; Abdelraheim, S. R.; Brazier, M. W.; Rigby, S. E. J.; Brown, D. R.; Viles, J. H. *Free Radical Biol. Med.* **2007**, *42*, 79–89.
- (52) Skvortsov, A. N.; Zavodnik, V. E.; Stash, A. I.; Bel'skii, V. K.; Skvortsov, N. K. *Russ. J. Org. Chem.* **2003**, *39*, 170–175.
- (53) Davis, A. V.; O'Halloran, T. V. *Nat. Chem. Biol.* **2008**, *4*, 148–151.
- (54) Camponeschi, F.; Valensin, D.; Tessari, I.; Bubacco, L.; Dell'Acqua, S.; Casella, L.; Monzani, E.; Gaggelli, E.; Valensin, G. *Inorg. Chem.* **2013**, *52*, 1358–1367.
- (55) Iwai, A.; Masliah, E.; Yoshimoto, M.; Ge, N.; Flanagan, L.; Rohan de Silva, H. A.; Kittel, A.; Saitoh, T. *Neuron* **1995**, *14*, 467–475.
- (56) Gruschus, J. M.; Yap, T. L.; Pistolesi, S.; Maltsev, A. S.; Lee, J. C. *Biochemistry* **2013**, *52*, 3436–3445.
- (57) Hopt, A.; Korte, S.; Fink, H.; Panne, U.; Niessner, R.; Jahn, R.; Kretzschmar, H.; Herms, J. *J. Neurosci. Methods* **2003**, *128*, 159–172.
- (58) Scheiber, I. F.; Mercer, J. F.; Dringen, R. *Prog. Neurobiol.* **2014**.
- (59) Burré, J.; Sharma, M.; Tsetsenis, T.; Buchman, V.; Etherton, M. R.; Südhof, T. C. *Science* **2010**, *329*, 1663–1667.
- (60) Schlieff, M. L.; Gitlin, J. D. *Mol. Neurobiol.* **2006**, *33*, 81–90.
- (61) Yang, L.; McRae, R.; Henary, M. M.; Patel, R.; Lai, B.; Vogt, S.; Fahrni, C. J. *Proc. Natl. Acad. Sci. U.S.A.* **2005**, *102*, 11179–11184.
- (62) Chavarría, C.; Souza, J. M. *Arch. Biochem. Biophys.* **2013**, *533*, 25–32.
- (63) Schildknecht, S.; Gerding, H. R.; Karreman, C.; Drescher, M.; Lashuel, H. A.; Outeiro, T. F.; Di Monte, D. A.; Leist, M. *J. Neurochem.* **2013**, *125*, 491–511.
- (64) Cole, N. B.; Murphy, D. D.; Lebowitz, J.; Di Noto, L.; Levine, R. L.; Nussbaum, R. L. *J. Biol. Chem.* **2005**, *280*, 9678–9690.
- (65) Zhou, W.; Long, C.; Reaney, S. H.; Monte, D. A. D.; Fink, A. L.; Uversky, V. N. *Biochim. Biophys. Acta* **2010**, *1802*, 322–330.
- (66) Uversky, V. N.; Yamin, G.; Souillac, P. O.; Goers, J.; Glaser, C. B.; Fink, A. L. *FEBS Lett.* **2002**, *517*, 239–244.
- (67) Glaser, C. B.; Yamin, G.; Uversky, V. N.; Fink, A. L. *Biochim. Biophys. Acta* **2005**, *1703*, 157–169.
- (68) Hokenson, M. J.; Uversky, V. N.; Goers, J.; Yamin, G.; Munishkina, L. A.; Fink, A. L. *Biochemistry* **2004**, *43*, 4621–4633.
- (69) Maltsev, A. S.; Chen, J.; Levine, R. L.; Bax, A. *J. Am. Chem. Soc.* **2013**, *135*, 2943–2946.
- (70) Martinez-Vicente, M.; Talloczy, Z.; Kaushik, S.; Massey, A. C.; Mazzulli, J.; Mosharov, E. V.; Hodara, R.; Fredenburg, R.; Wu, D.-C.; Follenzi, A. *J. Clin. Invest.* **2008**, *118* (2), 777–788.
- (71) Wassef, R.; Haenold, R.; Hansel, A.; Brot, N.; Heinemann, S. H.; Hoshi, T. *J. Neurosci.* **2007**, *27*, 12808–12816.
- (72) Liu, F.; Hindupur, J.; Nguyen, J. L.; Ruf, K. J.; Zhu, J.; Schieler, J. L.; Bonham, C. C.; Wood, K. V.; Davissou, V. J.; Rochet, J.-C. *Free Radical Biol. Med.* **2008**, *45*, 242–255.
- (73) Shearer, J.; Szalai, V. A. *J. Am. Chem. Soc.* **2008**, *130*, 17826–17835.
- (74) Rice, M. E. *Trends Neurosci.* **2000**, *23*, 209–216.
- (75) Guilloureau, L.; Combalbert, S.; Sourmia-Saquet, A.; Mazarguil, H.; Faller, P. *ChemBioChem* **2007**, *8*, 1317–1325.
- (76) Cassagnes, L.-E.; Hervé, V.; Nepveu, F.; Hureau, C.; Faller, P.; Collin, F. *Angew. Chem.* **2013**, *52*, 11110–11113.

- (77) Schallreuter, K. U.; Rübsam, K.; Gibbons, N. C. J.; Maitland, D. J.; Chavan, B.; Zothner, C.; Rokos, H.; Wood, J. M. *J. Invest. Dermatol.* **2007**, *128*, 808–815.
- (78) Wang, Z.-Y.; Shimonaga, M.; Muraoka, Y.; Kobayashi, M.; Nozawa, T. *Eur. J. Biochem.* **2001**, *268*, 3375–3382.